Effect of alkali-earth ions on local structure of the $LaAlO_3$–$La_{0.67}A_{0.33}MnO_3$ (A = Ca, Sr, Ba) diluted solid solutions: ^{27}Al NMR studies

© E.V. Charnaya, Cheng Tien*, N.V. Chejina**, M.K. Lee*, S.Y. Sun*

Institute of Physics, St. Petersburg State University, St. Petersburg, Petrodvorets, 198504 Russia
* Department of Physics, National Cheng Kung University, Tainan, 70101 Taiwan
** Department of Chemistry, St. Petersburg State University, St. Petersburg, Petrodvorets, 198504 Russia

E-mail: charnaya@paloma.spbu.ru

(Received May 11, 2006)

^{27}Al Magic Angle Spinning (MAS) NMR was studied for diluted alkali-earth metal doped lanthanum manganite solid solutions in the lanthanum aluminate $(1-y)LaAlO_3$–$yLa_{0.67}A_{0.33}MnO_3$ (A = Ca, Sr, Ba) with y = 0, 2, 3, and 5 mol%. The spectra depended on the dopant species and showed higher substitutional ordering for the Ba containing mixed crystals. Magnetically shifted lines were observed in all solid solutions and were attributed to Al in the octahedral oxygen environment near manganese trivalent ions. Nonlinear dependences of their intensity were referred to the manganese-rich cluster formation. An additional MAS NMR line corresponding to aluminum at sites different from the octahedral site in pure $LaAlO_3$ was observed only in solutions doped with Ba. 3Q MAS NMR revealed the the broadening of this line is governed mainly by quadrupole coupling and allowed calculating the isotropic chemical shift.

The present work was supported by the National Science Council of Taiwan under Grant 93-2811-M-006-021.

PACS: 76.60.-k, 61.66.-f

Doped lanthanum manganites $La_{1-x}A_xMnO_3$ (A is an alkali-earth metal such as Ca, Sr, Ba) are of increasing scientific and technological interest since the discovery of a colossal magnetoresistance in suitably substituted members of this family (around $x = 0.3$), and, generally, due to their unusual magnetic and charge transport features (for a review see [1]). However, the physics driving these properties is still rather unclear. In particular, a remarkable difference in influence of various substituting alkali-earth ions on exotic phenomena in manganites (see [2–4] and references therein) is not quite understood. Realizing that intrinsic inhomogeneities and mixed-phase characteristics exist and might play a key role in manganites, a great deal of efforts was focused on investigation of their structure and charge carrier distribution. In this context, studies of strongly diluted solid solutions of substituted manganites in allied aluminates can provide additiional informations of use.

Here we present results of ^{27}Al Magic Angle Spinning (MAS) and Multi-Quantum (MQ) MAS NMR studies for the $(1-y)LaAlO_3$–$yLa_{0.67}A_{0.33}MnO_3$ solid solutions (A = Ca, Sr, Ba) with y = 0, 2, 3, and 5 mol% in the parent powder.

1. Experimental

Samples under study were prepared by the conventional ceramic route from appropriate stoichiometric amounts of oxides and alkali-earth carbonates. The reagents were mixed, hand milled and pelleted, then sintered in air at 1500°C for 50 h. The homogeneity and the structure of the resulting compounds were monitored with x-ray powder diffraction. The powder diffraction patterns of solid solutions contained only peaks by the cubic perovskite structure of $LaAlO_3$ [5,6] which, as had been shown earlier, is typical for such kind of diluted compounds [7,8]. The cell parameters were changed for no more than 0.15% in agreement with [9]. The Mn percentage in the solid solutions was obtained by the atomic absorption method using an AASSIN spectrometer. It was found to decrease slightly compared to the parent powders, the composition of the sintered samples is listed in Table. Magnetic susceptibility was also measured and was found to remain constant after sintering longer than 50 h [10–12]. For NMR studies the pellets were milled once more.

The ^{27}Al MAS and MQ MAS experiments for the samples under study were performed on a Bruker Avance400 NMR pulse spectrometer using a commercial 4 mm MAS probehead. The spectra were acquired at the Larmor frequency of 104.3 MHz. The experimental

Values of y in solid solutions $(1-y)LaAlO_3$–$yLa_{1-0.33}A_{0.33}MnO_3$ (A = Ca, Sr, Ba) obtained by chemical analysis. Relative accuracy of y is about 3%

A	2%	3%	5%
Ca	0.0152	0.0260	0.0468
Sr	0.0136	0.0194	0.0330
Ba	0.0142	0.0209	0.0349

conditions were about the same as upon studying mixed aluminum garnets [13,14]. The maximal spinning rate was 12 kHz. The $\pi/12$ single pulse was used to botain MAS spectra. The recycle delay was 20 s and was more than by a factor of 5 larger than the spin-lattice relaxation time for all NMR spectrum components. The spectra width was 36 kHz to observe the central transitions and 500 kHz to observe all spinning sidebands corresponding to the octahedral aluminum site. The backward linear prediction was used to facilitate the phase correction for sidebands. A three-pulse sequence $mp3qzqf.2d$ was applied to get the two-dimensional 3Q MAS spectra. The NMR spectra were referenced to the 1 M $AlCl_3$ aqueous solution.

2. Results

The ^{27}Al MAS spectra in the undoped lanthanum aluminate ($LaAlO_3$) and in solid solutions with maximal dopant concentration obtained at room temperature and at 12 kHz spinning rate are shown in Fig. 1. The $LaAlO_3$ MAS spectrum is similar to that observed for instance in [15]. It contains the central line and sidebands corresponding to the only octahedral aluminum site. The nearly cubic symmetry of the lanthanum aluminate structure is responsible for small electric field gradients at the aluminum site, the quadrupole coupling constant being evaluated using the „xedplot“ software provided by Bruker as $e^2qQ/h \approx (0.14 \pm 0.02)$ MHz is in a good agreement with [15] and previous single-crystal measurements [16]. The chemical shift for the octahedral aluminum site is equal to 11.7 ppm also in agreement with [15].

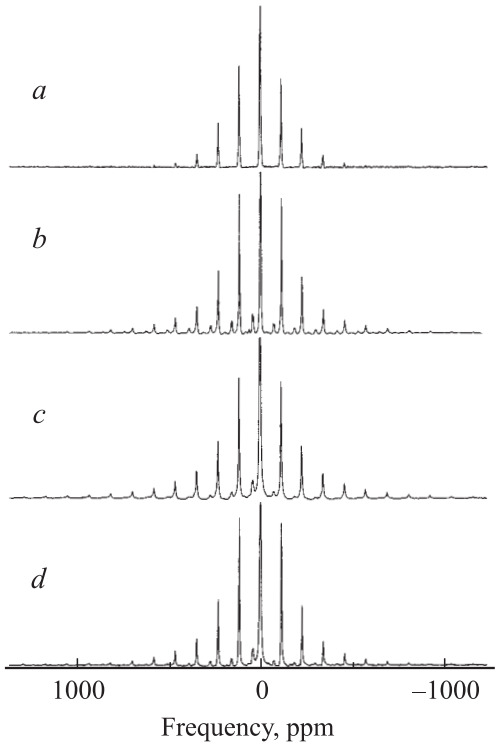

Figure 1. ^{27}Al MAS spectra at room temperature. Spinning rate is 12 kHz. a — spectrum in pure $LaAlO_3$. b, c, and d — spectra for Ba, Sr, and Ca containing solid solutions, respectively, at $y = 5\%$. The central lines in the spectra are cut at a level of 0.3 of their peak intensity.

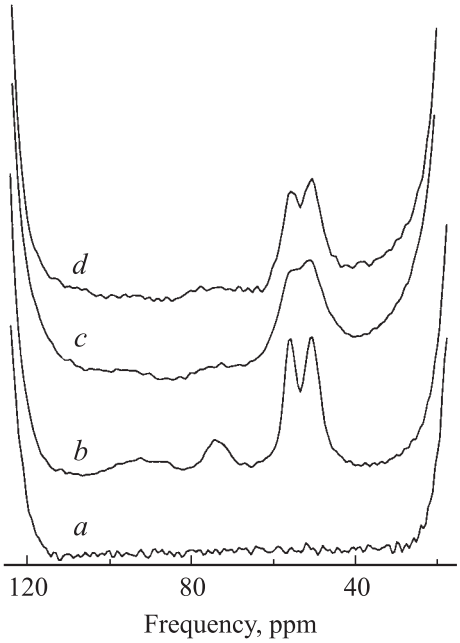

Figure 2. Central parts of ^{27}Al MAS spectra at room temperature. Spinning rate is 12 kHz. a — spectrum in pure $LaAlO_3$. b, c, and d — spectra for Ba, Sr, and Ca containing solid solutions, respectively, at $y = 5\%$.

The ^{27}Al MAS spectra for the solid solutions also contain the central line and sidebands appropriate to the octahedral aluminum site with envelopes slightly broadened compared to pure $LaAlO_3$. The quadrupole constants evaluated from the envelopes are then larger than in $LaAlO_3$ and are equal to (0.19 ± 0.02), (0.20 ± 0.02), and (0.18 ± 0.02) MHz for the samples doped with Ba, Sr, and Ca ($y = 5\%$), respectively. The chemical shift for the octahedral aluminum site was not changed within the accuracy of experiment.

Patterns for all doped samples show as well some additional lines as is seen from Fig. 2 for the central part of the ^{27}Al MAS spectra for the samples with $y = 5\%$. First, there is a line at about 45–60 ppm which is observed for all doped samples. This line has a shape typical for NMR lines broadened by anisotropic coupling. Assuming the quadrupole coupling as the main cause of the line broadening one can estimate the isotropic shift and the quadrupole constant using the „xedplot“ software, the isotropic shift being equal to 60 ppm and the quadrupole constant to 3.5 MHz. To clear the nature of the isotropic shift we conducted additional measurements of ^{23}Al MAS NMR spectra at several elevated and reduced temperatures between 200 and 325 K. The temperature during the measurement was stable within 0.5 K. The measurements showed that the isotropic shift with respect to Al in the

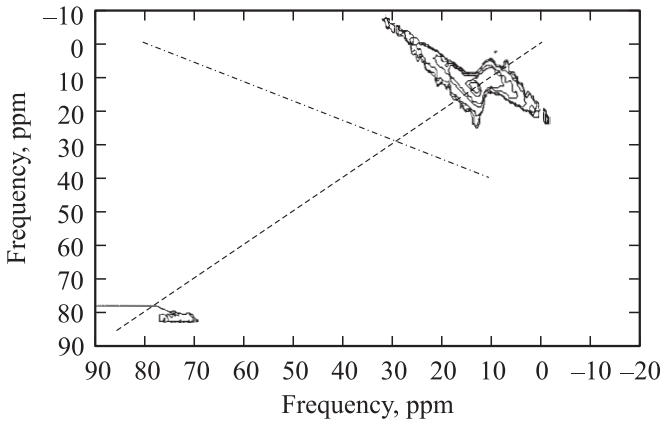

Figure 3. ^{27}Al 3Q MAS spectrum at room temperature for the Ba containing solid solution at $y = 5\%$. Dashed and dashed-dotted straight lines are the chemical shift and quadrupole-induced shift axes, respectively. Straight lines show the isotropic chemical shift evaluation for the additional aluminum site.

octahedral environment depends on temperature according to the $1/T$ law and thus is caused by magnetic coupling between Al at the octahedral site and Mn nuclei. Note that the line width did not depend noticeably on temperature in agreement with the quadrupoly origin of its broadening. Intensities of the magnetically shifted central lines were rather low (Fig. 2). Assuming the integral intensity of the central line from aluminum at the octahedral site equal to 1, the integral intensity of the magnerically shifted lines increased as 0.0.37 : 0.040 : 0.055, 0.021 : 0.033 : 0.068, and 0.049 : 0.051 : 0.065 when increasing y from 2 to 5% for the Ca, Sr, and Ba doped solid solutions, respectively.

Another additional line positioned at about 74 ppm can be reliably observed for the Ba-doped samples, only (Fig. 2, *b*). It does not move with changing temperature and its intensity does not depend on the Ba percentage within the experimental accuracy.

A 3Q MAS spectrum after shearing Fourier transformation for the Ba-doped sample at $y = 5\%$ is shown in Fig. 3. The chemical shift and quadrupole-induced shift axes are shown in Fig. 3 with dashed and dash-dotted lines. Two aluminum sites are clearly seen in Fig. 3: the octahedral site with the chemical shift 11.7 ppm and the additional site with the chemical shift 78 ppm. The magnetically shifted peak is not seen in the 3Q MAS spectrum. The top of the ridge corresponding to the octahedral aluminum sity lies on the chemical shift axis in agreement with a negligible quadrupole isotropic shift and small quadrupole constant. The ridge corresponding to the additional site in the Ba-doped samples is horizontally elongated. It shows that the relevant MAS NMR line is mainly broadened by anisotropic coupling and not because of the isotropic shift dispersion. According to Fig. 3, the isotropic quadrupole shift for this line is equal to — 4 ppm.

3. Discussion

In the solid solutions under study, the divalent Ca, Sr, and Ba ions with effective ionic radii $R_{Ca} = 0.99$, $R_{Sr} = 1.12$ and $R_{Ba} = 1.34$ Å substitute for the trivalent La ions with ionic radius $R_{La} = 1.15$ Å [17], while the Mn ions substitute for the smaller trivalent Al ions ($R_{Al} = 0.51$ Å) [7.9]. (The radii of the divalent Ca, Sr, and Ba ions and of trivalent La ions in the dodecahedral environment and those of trivalent Al in the octahedral environment differ from the effective values but only slightly [18].) When lanthanum aluminate is doped with only divalent cations like Ca, Sr, or Ba, oxygen ion vacancies are created for charge compensation [9]. On the other hand, in the $La_{1-x}A_xMnO_3$ concentrated solid solutions the deficit in positive charge is mostly made up by tetravalent manganese ions [1]. In the diluted solid solutions under study one could expect both kinds of charge compensation — oxygen vacancies and tetravalent manganese ions. However, experimentally we observed only one magnetically shifted central line in ^{27}Al MAS spectra of doped samples (Figs. 1, 2) which rises most probably due to trivalent menganese ions in the aluminum neighborhood. Thus, the charge compensation by oxygen vacancies plays an important role in the diluted solid solutions under study.

One can estimate the Fermi contact interaction caused by paramagnetic Mn ions using the observed isotropic shift in the solid solutions under study which seems to be independent of the dopant species (Fig. 2). The NMR shift δ in ppm induced by the Fermi contact interaction in materials with 3d metal ions is proportional to the unpaired electron spin density at the aluminum nucleus. This quantity at room temperature depends itself on the Fermi constant A_c and on the time-averaged value of the electron spin $\langle S_z \rangle$ [19]

$$\delta = -\frac{A_c}{\omega_0 \hbar} \langle S_z \rangle, \qquad (1)$$

where ω_0 is the Larmor frequency and $\hbar$ is the Planck constant. The time-average value can be calculated from $\langle S_z \rangle = -2A\mu_B B_0 / k_B T$ [20], where S is the total electron spin, μ_B is the Bohr magneton, B_0 is the external applied field, and k_B is the Boltzmann constant. For the trivalent Mn ions, S is equal to 2. Taking into account the value 48 ppm for the shift δ relative to the central line for Al in the octahedral site we have $A_c \cong 58$ kHz in the field 9.4 T at room temperature.

The composition dependences of the integral intensity of magnetically shifted lines mentioned in Section 3 do not scale with the Mn percentage listed in the Table. The increase in line intensities is noticeably slower than the increse in the amount of Mn ions, especially for the Ba-substituted solid solutions. The magnetic susceptibility measurements for diluted solid solutions carrier out in [10–12] revealed magnetic manganese-rich clusters containing the Mn^{3+} and Mn^{4+} ions, their number increasing with increasing y. NMR lines arising from aluminum nuclei in the neighborhood of such clusters should be broadened and

smeared and probably cannot be observed. Thus, the line positioned at 50–60 ppm is only due to aluminum ions far from the manganese-rich clusters. This justifies the weak increase of the magnetically shifted line intensity with increasing y.

Spectra depicted in Fig. 1 show the increase in the quadrupole constant for the doped samples which depended on the dopant species. Such increase can be hardly caused by alterations in the lattice parameters since they did not exceed 0.15% according to x-ray powder diffraction measurements. Then we should suggest that the ^{27}Al quadrupole constant increases because of minor lattice deformations due to substitutional disorder and to charge inhomogeneity in solid solutions which lead to lowering the high symmetry of the oxygen octahedra in pure $LaAlO_3$. Note, however, that while the ionic radius is maximal for the Ba^{2+} ions the quadrupole constant alteration for the Ba-doped sample is between the values for the Ca and Sr-containing solid solutions. As can be also seen from Fig. 2, the lines in ^{27}Al MAS spectra corresponding to the Ba-doped sample are the most narrow compared to other solid solutions. It means that the lattice and charge disorder is minimal in the barium substituted solid solutions. It is plausible that because of big ionic radius of the divalent Ba ions, there occures a trend to more homogeneous barium distribution over the dedecahedral lattice sites upon substituting the La^{3+} ions than in other solid solutions.

The origin of the additional line positioned at 74 ppm in the Ba-substituted solid solution (Fig. 2) is not quite clear. Its chemical isotropic shift (Fig. 3) falls into a chemical shift range specific for aluminum in tetrahedral oxygen nearest neighborhood (see, for instance [21,22]). While such tetrahedral sites are prohibited by crystalline structure of the samples under study, one cannot exclude the formation of submicroheterogeneities with the structural motives of $LaBaAlO_4$, in which Al is in the tetrahedral oxygen neighborhood. The removal of an oxygen ion in the barium neighborhood could make a quasi tetrahedral surrounding for aluminum with one more oxygen at a greater distance just like it occurs in the $CaSO_4$-type structure of $LaBaAlO_4$. The situation seems to remind that in $Fe_{1-y}O$, where Fe^{3+} was found to move into tetrahedral sites thus forming the structural motives of spinel in the rock salt structure without noticeable disruption of homogeneity [23]. The regular structure of the $LaBaAlO_4$ motives agrees well with the narrow projection of the relevant $3Q$ MAS ridge onto the vertical axis in Fig. 3. Such a suggestion about the origin of the additional line in the Ba-substituted samples is the most plausible. However, we should also mention another possibility. For $YAlO_3$ doped with larger Ce ions, EPR data [24] suggested that some of Al ions move to the dodecahedral lattice sites in the Ce neighborhood. Similarly one could suggest that the line at about 74 ppm arises due to aluminum ions moved to the dodecahedral sites when the Ba ions with big radius substitute for lanthanum.

4. Conclusions

^{27}Al NMR studies of diluted alkali-earth doped lanthanum manganite solid solutions in lanthanum aluminate showed the highest substitutional order in the Ba containing samples. The magnetically shifter line in NMR spectra for the solid solutions was referred to aluminum at the octahedral sites in the neighborhood of Mn^{3+} ions, its nonlinear dependence on the Mn percentage being related with formation of magnetic manganese-rich clusters. Another additional line positioned at about 74 ppm was observed only in the spectra of Ba-substituted solutions. The formation of submicroheterogeneities of the $LaBaAlO_4$ structural motives with aluminum ions in tetrahedral sites was suggested as the most plausible origin of this line.

References

[1] E. Dagotto, T. Hotta, A. Moreo. Phys. Rep. **344**, 1 (2001).
[2] P. Mandal, B. Ghosh. Phys. Rev. B **68**, 014 422 (2003).
[3] J.M.D. Coey, M. Viret, S. von Molnar. Adv. Phys. **48**, 167 (1999).
[4] T. Chatterji, L.P. Regnault, W. Schmidt. Phys. Rev. B **66**, 214 408 (2002).
[5] S. Geller, V.B. Bala. Acta Crystallogr. **9**, 1019 (1956).
[6] S. Bueble, K. Knorr, E. Brecht, W.W. Schmahl. Surf. Sci. **400**, 345 (1998).
[7] Б.Я. Брач, Б.Н. Дудкин, И.И. Кожина, Н.В. Чежина. Кристаллография минералов. Наука, Л. (1981).
[8] P.S. Anderson, F.M.B. Marques, D.C. Sinclair, A.R. West. Solid State Ionics **118**, 229 (1999).
[9] J.W. Fergus, C.B. Alcock. Mater. Lett. **12**, 219 (1991).
[10] N. Chezhina, M. Mikhailova, A. Osipova. Solid State Ionics **141–142**, 617 (2001).
[11] Н.В. Чежина, М.В. Кузьмин. ЖОХ **72**, 871 (2001).
[12] Н.В. Чежина, М.В. Кузьмин. ЖОХ **74**, 535 (2004).
[13] E.V. Charnaya, C. Tien, J.J. Lu, R.R. Wu, S.N. Ivanov, E.N. Khazanov. J. Phys.: Condens. Matter. **13**, 8775 (2001).
[14] C. Tien, E.V. Charnaya, S.Y. Sun, R.R. Wu, S.N. Ivanov, E.N. Khazanov. Phys. Stat. Sol. (b) **233**, 222 (2002).
[15] R. Dupree, M.H. Lewis, M.E. Smith. J. Am. Chem. Soc. **111**, 5125 (1989).
[16] K.A. Müller, G. Burn, B. Derighetti, J.G. Drumheller, F. Waldner. Phys. Lett. **9**, 223 (1964).
[17] CRC Hand Book of Chemistry and Physics / Ed. D.R. Lide. CRC Press, Boca Raton (1996).
[18] R.D. Shannon, C.T. Prewitt. Acta Cryst. B **25**, 925 (1969).
[19] H.M. McConnell, R.E. Robertson. J. Chem. Phys. **29**, 1361 (1958).
[20] C. Kittel. Introduction to Solid State Physics. Wiley, N.Y. (1986).
[21] R. Hussin, D. Holland, R. Dupree. J. Non-Cryst. Solids **298**, 32 (2002).
[22] F. Taulelle, J. Maquet, V. Lucas et al. Appl. Magn. Res. **4**, 101 (1993).
[23] A.R. West. Solid State Chemistry and Its Applications. John Wiley and Sons, N.Y. (1986).
[24] H.R. Asatryan, J. Rosa, J.A. Mareš. Solid State Commun. **104**, 5 (1997).